ALIX AND ALG-2 ARE INVOLVED IN TNF-R1 INDUCED CELL DEATH

Anne-Laure Mahul-Mellier [1,4,5], Flavie Strappazzon[1,4,6], Anne Petiot[1,4], Christine Chatellard-Causse[1,4], Sakina Torch[1,4], Béatrice Blot[1,4], Kimberley Freeman [1,4], Loriane Kuhn [2,3,4], Jérome Garin [2,3,], Jean-Marc Verna[1,4], Sandrine Fraboulet[1,4,7], Rémy Sadoul[1,4]

INSERM, U836, Equipe 2, Neurodégénérescence et Plasticité, Grenoble, F-38042, France[1]. CEA, DSV, iRTSV, Laboratoire d'Etude de la Dynamique des Protéomes, Grenoble, F-38054, France[2]. INSERM, U880, Grenoble, F-38054, France[3]. Université Joseph Fourier, Grenoble Institut des Neurosciences, Grenoble, F-38042, France[4]

Present addresses : Imperial College London, Experimental Medicine & Toxicology, London W120NN[5]. European Center for Brain Research, Santa Lucia Foundation, Molecular Neuroembryology Unit, 00143, Rome, Italy[6]. MRC Functional Genetic Unit, University of Oxford, Department of Physiology Anatomy and Genetics, OX1 3QX Oxford, UK[7]

Address correspondance to: Rémy Sadoul, Grenoble Institute of Neuroscience, Chemin Fortuné Ferrini, BP 170, F- 38042 Grenoble, France. tel: ++33 456 52 05 44, email: remy.sadoul@ujf-grenoble.fr and Sandrine Fraboulet, Le Gros Clark Building University of Oxford South Parks Road Oxford OX1 3QX,UK. tel: +44 1865 282 273, email: sandrine.fraboulet@dpag.ox.ac.uk

Alix/AIP1 regulates cell death in a way involving interactions with the calcium binding protein ALG-2 and with proteins of the *endosomal sorting complex required for transport* (ESCRT). Using mass spectrometry we identified caspase-8 among proteins co-immunoprecipitating with Alix in dying neurons. We next demonstrated that Alix and ALG-2 interact with pro-caspase-8, and that Alix forms a complex with the TNFα receptor-1 (TNF-R1), depending on its capacity to bind ESCRT proteins. Thus, Alix and ALG-2 may allow the recruitment of pro-caspase-8 onto endosomes containing TNF-R1, a step thought to be necessary for activation of the apical caspase. In line with this, expression of Alix deleted of its ALG-2 binding site (AlixΔALG-2) significantly reduced TNF-R1 induced cell death, without affecting endocytosis of the receptor. In a more physiological setting, we found that programmed cell death of motoneurons, which can be inhibited by AlixΔALG-2, is regulated by TNF-R1. Taken together, these results define Alix and ALG-2 as regulators of the TNF-R1 cell death pathway.

Endocytosis of cell surface receptors has long been described as an effective way of switching off extracellularly induced signals. Endocytosed activated receptors traffic through early endosomes and are sorted into intralumenal vesicles accumulating inside endosomes known as multivesicular bodies (MVBs). These MVBs fuse with lysosomes where the receptors meet their end by acid hydrolysis (1).

In some cases however, such as for neurotrophin bound Trk receptors, activated receptors continue signalling inside endosomes (2). Also, in the case of death receptors, Schütze and colleagues showed that endocytosis of TNF-R1, which occurs after binding to TNFα, is a necessary step for activation of caspases and consequently apoptosis. They found that the apical pro-caspase-8 is recruited and thereby activated on the surface of multivesicular endosomes containing activated TNF-R1 (3).

Biogenesis of MVBs is under tight control by a set of proteins, making the so-called *endosomal sorting complexes required for transport* (ESCRT-0 to -III), which sequentially associate on the cytosolic surface of endosomes (4). A partner of ESCRT proteins, which also regulates the making of MVBs, is the protein Alix/AIP1, first characterised as an interactor of the calcium binding protein ALG-2 (Apoptosis Linked Gene-2) (5-7). Enveloped viruses, like HIV-1, use Alix to recruit the ESCRT machinery in order to deform membranes and allow fission during viral budding (8,9). Furthermore, two recent reports have claimed that Alix together with ESCRT proteins might also be involved in the abscission stage of cytokinesis (10,11).

Besides Tsg101 and CHMP-4B of ESCRT-I and III respectively, Alix interacts with lysobisphosphatidic acid (LBPA), a phospholipid involved in intralumenal vesiculation of endosomes (12), and with regulators of endocytosis (CIN85 and

endophilins) (13,14). However, the precise role of Alix on endosomes remains largely unclear as neither we nor other laboratories have found any striking effect of Alix on endocytosis and degradation of EGF or transferrin receptors (15,16).

Alix may play a role in cell death. In particular, expression of a mutant lacking the N-terminal part (Alix-CT) blocks death of Hela cells induced by serum starvation (7) and of cerebellar neurons deprived of potassium (17). In this latter paradigm, Alix-CT whose protecting activity was strictly correlated with its capacity to bind ALG-2, accumulated inside cytoplasmic aggregates together with ALG-2 and caspases. We also demonstrated, using electroporation in the chick embryo, that Alix mutants block programmed cell death of motoneurons during normal development, depending on binding to ALG-2, ESCRT-I and III. Our interpretation of these results is that some truncated forms of Alix behave as dominant negative mutants blocking the formation of an ALG-2/Alix/ESCRT complex necessary for cell death (18). Therefore the Alix/ALG-2 complex could make a link between endosomes and a signalling- or an execution step of neuronal death (19).

We have undertaken the present study to characterise this link and found that Alix and ALG-2 form a complex with endocytosed TNF-R1 and pro-caspase-8. Testing the physiological significance of these interactions both *in vivo* and *in vitro* allowed us to define Alix/ALG-2 as a new controller of TNF-R1 induced cell death.

Experimental procedures

Reagents and antibodies

Human recombinant TNFα-Flag was from Alexis biochemicals (Covalab, France). Mouse monoclonal anti-haemagglutinin (HA) antibody was from Cell Signaling (Ozyme, France); polyclonal antibodies against Myc, TNF-R1 and FADD were from Santa Cruz Biotechnology (Germany); polyclonal antibodies against LAMP1 and EEA1 were from AbCam (France); anti-Flag monoclonal (M1 and M2) and polyclonal antibodies from Sigma-Aldrich (France); GM130 and monoclonal anti-AIP1/Alix was from BD Transduction (France); anti-ALG-2 was from Swant (Switzerland); HSP70 mitochondria was from Affinity Bioreagents (Ozyme, France); anti-caspase 8 was from Biovision (Clinisciences, France); horseradish peroxidase-conjugated goat anti-mouse and anti-rabbit Alexa^{594} antibody from Jackson Laboratories (USA); biotinylated goat anti-rabbit antibody from Vector Laboratories, (USA).

DNA constructs

For expression in the chick embryo, human TNF-R1 (wt or mutants), a catalytically dead version of human pro-caspase-8 (mutation C360A), and baculovirus p35 were inserted into the pCAGGS expression vector (a gift of Tsuyoshi Momose; Nara Institute of Science and Technology, Japan). Mammalian expression vectors coding for DN-caspase-8-HA-Tagged and p35 were a gift of P.Mehlen (Inserm Lyon, France). Those coding for wt or mutated human TNF-R1 were kind gifts from W. Schneider-Brachert (University of Regensburg, Germany). Mutated ALG-2ΔEF^{1,3} was a gift of M. Maki (Nagoya University, Nagoya, Japan).

In ovo electroporation

Fertilised Isa Brown eggs (Société Française de Production Avicole, St Marcellin, France) were electroporated at Hamburger Hamilton (HH) stage 16. Plasmid DNA was electroporated as described in (18).

Histological analysis

Chick embryos were collected 48h after electroporation processed and cryo-sectioned as described previously in (18).

Immuno-histochemistry and –fluorescence

Frozen sections were incubated with polyclonal anti-TNF-R1 or monoclonal anti-HA antibodies, diluted to 1/100 in Tris Buffer Saline containing 1% GS/0.02% saponine (TBSS) for 12 to 24 hours at 4°C. Sections were rinsed in TBSS and treated with a secondary anti-rabbit Alexa^{594} antibody or a biotinylated goat anti-rabbit secondary antibody, amplified using the ABC kit (Vector Laboratories, USA) and revealed with 3,3'-diaminobenzidine (DAB) and nickel intensification. Sections were rinsed in TBS, incubated 30 minutes at 37°C in Hoechst 33342, 2 μg/ml (Sigma, France), before mounting in Mowiol (Calbiochem, France).

Terminal deoxynucleotidyl transferase-mediated dUTP-biotin nick end labelling (TUNEL) method

TUNEL analysis were performed using the In Situ Cell Death Detection kit (Roche, France). Fluorescent positive cells were

counted in every third section. Twelve sections per embryo were counted.

RT-PCR

RNA were extracted from whole chick embryo using Trizol reagent (Invitrogen). cDNAs were synthesised with MMLV-RT (Promega, France) and controlled with GAPDH. TNF-R1 expression was further analysed by amplification of a 695 nt fragment with the following oligonucleotides:

5'GATACTGTGTGTGGCTGT3'and

5'CGTAAATGTCGATGCTCC3' based on the chick TNF-R1 homologue (Gallus gallus accession number AJ720473).

Cell culture and transfection

HEK-293 cells were maintained in DMEM (Invitrogen, France) containing 10% foetal bovine serum (FBS) (Invitrogen, France), 2 mM glutamine, 10 µg/ml streptamycine and 10 U/ml penicilline. BHK-21 cells were maintained in G-MEM (Invitrogen) containing 5% FBS, 2.6 g/L tryptose phosphate broth, 2 mM glutamine, 10 µg/ml streptamycine and 10 U/ml penicillin. HEK 293 or BHK-21 cells were transfected using JetPEI (Ozyme, France).

Alix Knock-down in BHK cells

The Alix shRNA was cloned downstream of the human H1 promoter in the vector pSuperGFP (Oligoengine, USA). The sequences of the synthetic oligonucleotides (Invitrogen) used for Alix shRNA construct were the following:

5'GATCCCCGCCGCTGGTGAAGTTCAT CTTCAAGAGAGATGAACTTCACCAGCG GCTTTTTGGAAA3' and

5'AGCTTTTCCAAAAAGTTCATCCAGC AGACTTACTCTCTTGAAGTAAGTCTGCT GGATGAACGGG3'

Annealed oligonucleotides were ligated into the BglII cleavage site within the pSuperGFP vector linearised with the same restriction enzymes.

BHK cells were transfected with pSuper/shAlix plasmid or pSuperGFP vector for control using the JetSi transfection reagent (Polyplus tranfection, France). Transfected cells were selected using 800 µg/ml of G418. After 15 days, clones were isolated and selected for the best reduction in Alix expression. Cells (pSuper/shAlix and control) were grown in presence 800 µg/ml of G418.

Mass spectrometry and Protein identification

Cultures of mouse cerebellar granule neurons were prepared as described previously (Trioulier *et al*., 2004) and cultured in BME containing 25 mM potassium. Medium was changed for BME containing 5 mM potassium and cells were lysed 4 hours later in RIPA buffer buffer (150 mM NaCl, 50 mM Tris pH 8.0, 1% NP-40, 0.5% deoxycholate, 0.1% SDS containing a protease inhibitor mixture (Roche, France). Immunoprecipitations were performed using polyclonal-anti-Alix antibody and protein-G coupled Sepharose beads. After separation by SDS-PAGE, discrete bands were excised from the Coomassie blue-stained gel. In-gel digestion was performed as previously described (41). Gel pieces were then sequentially extracted with 5% (vol/vol) formic acid solution, 50% acetonitrile, 5% (vol/vol) formic acid, and acetonitrile. After drying, the tryptic peptides were resuspended in 0.5% aqueous trifluoroacetic acid. For MALDI-TOF-MS analyses, a 0.5 µL aliquot of peptide mixture was mixed with 0.5 µL matrix solution (cyano-4-hydroxycinnamic acid at half saturation in 60 % acetonitrile / 0.1 % trifluoroacetic acid (TFA) (vol/vol)). The resulting solution was spotted on a MALDI-TOF target plate, dried and rinsed with 2µL of 0.1 % TFA. Peptide mixtures were then analysed with a MALDI-TOF mass spectrometer (Autoflex, Bruker Daltonik, Germany) in reflector/delayed extraction mode over a mass range of 0-4200 Da. Spectra were annotated (XMass software) and the peptide mass fingerprints obtained were finally submitted to database searches against the Swissprot Trembl database with an intranet 1.9 version of MASCOT software.

Immunoprecipitation and Western blotting

Twenty-four hours after transfection, HEK-293 or BHK-21 were lysed in RIPA. Cell lysates were cleared by a 14 000 g centrifugation for 15 min, and incubated overnight at 4°C with anti-Flag monoclonal M2 Ab. Immune complexes were precipitated with protein G-Sepharose (Amersham Biosciences, France) and the beads washed with RIPA buffer. Immunoprecipitated proteins were separated by 10% SDS-PAGE and transferred onto a PVDF membrane (Millipore, France). Membranes were blocked with 5% milk in TBS containing 0.1% Tween and incubated with the appropriate antibodies. Bands were revealed using the ECL detection reagent (Perbio, France).

In the case of immunoprecipitation between endogenous Alix and TNF-R1, HeLa cells

were lysed in RIPA buffer. Cell lysates were cleared by a 14 000 g centrifugation for 15 minutes followed by two incubations of 30 min with protein G-Sepharose beads. Cell lysates containing 5 mg total proteins were incubated 1h at 4°C with the polyclonal antibody against TNF-R1. Immune complexes were precipitated with protein G-Sepharose (Amersham Biosciences, France) and the beads washed with RIPA buffer. Immunoprecipitated proteins were separated by 8% SDS-PAGE and treated as described above. Alix was detected using the monoclonal anti-AIP1/ Alix from BD transduction laboratories.

Quantification of cell death induced by TNF-R1

Twenty hours after transfection, HEK-293 were washed in PBS, pH 7.4 and fixed in 4% paraformaldehyde for 20 min at 4°C. Cells were stained with polyclonal anti-TNF-R1 antibody (1/100) and anti-rabbit Alexa^{594} antibody (1/500). Cells were rinsed in TBS, incubated for 30 minutes at 37°C in 2 µg/ml Hoechst 33342 (Sigma) and mounted in Mowiol. Cell viability was scored on the basis of nuclear morphology, condensed or fragmented nuclei being counted as dead.

In some cases, tetrazolium salt MTT (Sigma, France) was added to cells at a final concentration of 1 mg/ml and incubated for 30 min at 37 °C. Dimethyl sulfoxide was used to dissolve the formazan product and absorbance was measured in each well at 540 nm, using a measure at 630 nm as reference, in a Biotek El_x-800 microplate reader (Mandel Scientific Inc, Canada).

TNFα internalisation

BHK cells co-expressing TNF-R1 and the indicated proteins, were incubated for 1 h at 4°C with 1 ng ^{125}I-labelled human recombinant TNFα (specific activity 2160 kBq/µg) (NEN Life Science Products, PerkinElmer LAS, France). Cells were then incubated at 37°C to allow endocytosis for the indicated times. The amount of intracellular ^{125}I-TNF receptor complexes formed at 37°C was estimated after washing cells for 5 minutes in cold acetic acid buffer (200 mM acetic acid, 500 mM NaCl pH 2.5). After two washes in PBS, cells were lysed in RIPA buffer. Total amount of cell-associated ^{125}I-TNFα was determined on cells, washed only with PBS, instead of the acetic acid buffer. The amount of internalised (pH 2.5 resistant) ^{125}I-TNF was calculated as a percentage of ^{125}I-TNF bound at pH 7.4.

Magnetic isolation of endosomes containing TNF-R1 bound to TNFα

HEK 293 cells, transfected with TNF-R1 and Alix-Myc were incubated in a total volume of 1 ml of cold D-PBS (0.9 mM $CaCl_2$, 0.493 mM $MgCl_2$, 2.67 mM KCl, 1.47 mM KH_2PO_4, 138 mM NaCl, 8 mM Na_2HPO_4) containing 3% BSA, 100 ng/ml TNFα-Flag and 10 µg/ml anti-Flag monoclonal M1 for 1 h at 4°C. They were then washed twice in cold D-PBS and incubated for 1 h at 4°C in 1ml cold D-PBS containing 50 µl of protein G microbeads (µMACS Protein G Microbeads, MACS Molecular, Miltenyi Biotec, France). Cells were then washed twice in cold D-PBS and incubated in DMEM containing 10% SVF and kept at 4°C, or incubated for 30 minutes at 37°C. Removal of surface bound M1 antibody was achieved by washing the cells three times 5 minutes in cold PBS containing 1mM EDTA. A post-nuclear supernatant was prepared in 8% sucrose supplemented in 3 mM imidazole, pH 7.4 and 2X protease inhibitor mixture (Gruenberg *et al.*, 1989). The magnetic immune complex was passed over a column placed in the magnetic field of a MACS Separator. The labelled TNFα receptosome was retained within the column while unbound material was washed away with 8% sucrose, 3mM imidazole pH 7.4. The magnetic fractions were collected by removing the column from the magnetic field and analysed by SDS-PAGE and Western blotting. Solubilisation of endosomes was performed using a solution of 8% sucrose, 3mM imidazole, pH 7.4, containing 0.5 % Triton-X100.

RESULTS

Alix interacts with pro-caspase-8 through ALG-2.

In order to understand how Alix might control cell death, we first characterised some of the proteins interacting with it during apoptosis. For this, we used cerebellar granule cells, which survive in absence of serum when cultured in high extracellular potassium (25 mM) but undergo apoptosis soon after they are incubated in a medium containing normal extracellular potassium concentrations (5

mM). We previously observed that expression of Alix-CT blocks caspase activation in neurons deprived of potassium (17). We used a polyclonal anti-Alix antibody to immunoprecipitate the endogenous protein from cell lysates made from neurons incubated for 4 hours in 5 mM potassium. Using peptide mass fingerprinting (see Materials and Methods), we found caspase-8 among the proteins co-immunoprecipitated with Alix, suggesting that the protease may physically associate with Alix. We further showed that in BHK-21 cells, Flag-tagged-Alix (Flag-Alix) and an HA-tagged-, catalytically inactive version, of pro-caspase-8 (HA-DN-pro-caspase-8) (Figure 1) co-immunoprecipitated. This demonstrates that the two proteins exist in a complex and that activity of the caspase is not required for this interaction (Figure 2A). Furthermore, deletion of the prodomain of pro-caspase-8 containing the two DED domains abolished the capacity of the caspase to interact with Alix (Figure 2B). Addition of 1 mM Ca^{2+} in the lysates strikingly enhanced the amount of Alix co-immunoprecipitating with pro-caspase-8 (Figure 2A) and we detected endogenous ALG-2 in immunoprecipitates containing overexpressed Alix and pro-caspase-8 (Figure 2C). This prompted us to test a potential interaction of pro-caspase-8 with ALG-2, whose binding to Alix depends on calcium. In the case where ALG-2 was co expressed with DN-pro-caspase-8, ALG-2 co-immunoprecipitated with the caspase in presence of 1 mM $CaCl_2$ (Figure 3A). Here again, this interaction required the pro-domain of the caspase (Figure 3B). Flag-Alix deleted of the sequence P^{802}PYPTYPGYPGY^{813} necessary for the binding of ALG-2 (17) (AlixΔALG-2) (Figure 1) did not immunoprecipitate with DN-pro-caspase-8 (Figure 3C). On the other hand, ALG-2 could be co-immunoprecipitated with DN-pro-caspase-8 equally well from lysates of wt BHK cells or from cells in which Alix expression had been down regulated using a pSuper vector coding for an shRNA against Alix, indicating that ALG-2 can interact with pro-caspase-8 independently of Alix (Figure 3D).

Alix immunoprecipitates with TNF-R1 independently of ALG-2.

The demonstration that TNF-R1 needs endocytosis to recruit pro-caspase-8 prompted us to test whether Alix and ALG-2 act as adaptors bringing pro-caspase-8 into close vicinity of endosomes containing TNF-R1. First, we examined whether Alix and ALG-2 can form a complex with TNF-R1.

These experiments were performed in HEK 293 cells transiently transfected with expression vectors coding for TNF-R1 and Alix. As reported (20), TNF-R1 overexpression was sufficient to induce apoptosis, even in absence of TNFα. Western blot analysis of Alix or TNF-R1 immunoprecipitates (Figure 4A and not shown) revealed the presence of TNF-R1 and Alix respectively, suggesting the existence of a complex containing both proteins. We further proved the existence of such a complex by showing that endogenously expressed Alix is pulled down with endogenous TNF-R1 immunoprecipitated from Hela cells (Figure 4B). In HEK 293 cells, TNF-R1 mutant deleted of the death domain (TNF-R1ΔDD) (Figure 1) did not co-immunoprecipitate with Alix, indicating that the interaction depends on the integrity of this region (Figure 4C). AlixΔALG-2, which does not interact with pro-caspase-8, was capable of co-immunoprecipitating with TNF-R1 (Figure 4C). This underscores the fact that binding of Alix to a TNF-R1 complex is independent of ALG-2 and of pro-caspase-8. Interestingly, Alix mutants lacking the Bro1 domain, required for interaction with CHMP-4B, or four amino acids necessary for binding to Tsg101, were not capable of co-precipitating with TNF-R1 (Figure 4D). Thus, co-immunoprecipitation of Alix with TNF-R1 requires its ability to bind ESCRT proteins.

ALG-2 immunoprecipitates with TNF-R1 in a way which tightly depends on its capacity to bind calcium.

We next asked whether ALG-2 can associate to TNF-R1. Lysates from HEK 293 cells co-transfected with Flag-ALG-2 and wild-type TNF-R1 expression vectors were immunoprecipitated with anti-Flag (Figure 5A) or with anti-TNF-R1 antibodies (not shown). In both cases, Western blots revealed co-immunoprecipitation of TNF-R1 with ALG-2. Furthermore, endogenous Alix was detected in the ALG-2 immunoprecipitates containing TNF-R1 (Figure 5A).

We also used a mutated form of ALG-2, ALG-2ΔEF^{1,3}, harbouring point mutations in the first and third EF hands which abolish its capacity to bind calcium. In accordance to

published observations (21), this calcium binding- deficient ALG-2 did not co-immunoprecipitate with Alix (Figure 5Ba). ALG-2ΔEF^{1,3} was also unable to interact with TNF-R1, stressing the fact that ALG-2 must be able to bind Ca^{2+} in order to co-immunoprecipitate with TNF-R1 (Figure 5Bb). These results show that even though formation of a complex containing TNF-R1/Alix does not necessitate interaction with ALG-2, the latter bound to calcium can associate with it, possibly by binding to Alix.

Alix is associated with TNF-R1 receptosomes

Our observation that deletion of ESCRT interacting domains from Alix impairs its capacity to bind to TNF-R1 containing complexes, could suggest that interaction of the protein with the TNF-R1 complex occurs on endosomes. To examine this possibility, we used magnetic beads coupled to protein G to immuno-isolate TNFα containing endosomes, a method modified from that published by Schütze and colleagues (3): Flag tagged-TNFα was applied to HEK 293 cells overexpressing TNF-R1 at 4°C in presence of M1, an anti-Flag antibody binding only in presence of calcium. Cells were incubated at 37°C for 30 minutes to allow endocytosis and then treated briefly with EDTA to remove surface bound antibody. The resulting immuno-isolated membrane fractions contained TNF-R1, two markers of endosomes, EEA1 and Lamp-1, but neither the mitochondrial marker HSP70, nor cis-Golgi marker GM130, stressing the endosomal origin of these fractions (Figure 6A). None of the proteins tested could be detected in magnetic particles recovered from cells left at 4°C and treated with EDTA (Figure 6A, lanes 0), thus demonstrating the efficiency of the washing procedure for removing the M1 anti-Flag antibody from TNFα bound to TNF-R1 remaining on the cell surface.

Triton X-100 solubilisation of the endosomal membranes, witnessed by the loss of EEA1 and Lamp-1 labelling, left intact TNF-R1, Alix, ALG-2, pro-caspase-8, and FADD-immunoreactivity (Figure 6B). This result indicates that these proteins interact within complexes containing endocytosed TNF-R1 bound to TNFα.

AlixΔALG-2 protects HEK 293 cells from TNF-R1 induced cell death without affecting internalisation of the receptor.

HEK 293 cells die soon after transfection with an expression vector coding for TNF-R1 but not with one encoding TNF-R1ΔDD (Figure 7Aa). Blocking clathrin-dependent endocytosis by a dominant negative mutant of dynamin 2a, significantly reduced TNF-R1 induced cell death (Figure 7Aa). AlixΔALG-2, which interacts with TNF-R1 but not with pro-caspase-8, inhibited cell death induced by TNF-R1, estimated by Hoechst nuclear staining (Figure 7Ab) and MTT-assay (Figure 7B). Alix-wt or AlixΔTSG101, which cannot interact with TNF-R1, did not protect against TNF-R1-induced cell death (Figure 7Ab).

Using [^{125}I] radiolabelled TNFα we found no difference in TNFα internalisation between TNF-R1 overexpressing cells co-transfected with control plasmid, Alix or AlixΔALG-2, whereas internalisation was abolished by co-transfection with a dominant negative mutant of dynamin 2a (Figure 7C). These results indicate that the protective effect of AlixΔALG-2 is not due to blockade of receptor internalisation.

AlixΔALG-2 blocks cell death of cervical motoneurons which is regulated by TNF-R1.

We finally tested whether the participation of Alix and ALG-2 in the TNF-R1 death pathway demonstrated *in vitro* may also apply *in vivo*. For this we searched whether programmed cell death of cervical motoneurons (MTN) in the chick embryo, which is efficiently blocked by expression of AlixΔALG-2 (18), depends on TNF-R1. RT-PCR analysis revealed expression of the TNF-R1 mRNA in whole chick embryo extracts from HH stage 16 to HH stage 27 (Figure 8A). We next used a polyclonal antibody, raised against the extracellular part of human TNF-R1, which we verified to recognize the chick counterpart (40.5% identity on the 222 extracellular amino-acids). Indeed, the antibody revealed bands at the expected 55 kD in blots prepared from chick fibroblasts (DF1 cell line) and chick embryo extracts (Figure 8B). Immunostaining revealed expression of TNF-R1 in the dermomyotome but not in the neural tube of HH stage 16 chick embryo. Labelling of the ventral-most part of the ventral horn and of MTN axons growing out of the tube was detected at HH stage 21 and 24 (Figure 8C-D), and decreased at HH stage 27 (not shown).

Taken together, these results show that TNF-R1 is transiently expressed in MTN during a short period corresponding to that of programmed cell death. In comparison, Alix is expressed in the same areas of the neural tube but appearing earlier (HH stage 16) and for longer during development (22).

We first tested the involvement of caspase-8 during death of MTN, using electroporation of the chick neural tube. This technique allows expression of the protein of interest in one half of the embryo, the other half being left intact for comparison. p35, a baculovirus protein inhibiting most caspases (23), was electroporated into the cervical neural tube of HH stage 16 embryos which were sacrificed 48 hours later (Figure 9Aa). Comparison between transfected and non transfected ventral horns of the same embryo revealed a reduction by half of the number of TUNEL positive neurons in the p35 expressing ventral horn (Figure 9Ab and 9B). Using the same technique, we found that expression of DN-pro-caspase-8 (Figure 9Ac,d and 9B) also reduced the number of dying neurons to a similar degree as AlixΔALG-2 (18). This indicates a role of Alix/ALG-2 and of the death-receptor regulated apical caspase-8 in MTN programmed cell death during development.

Overexpression of human wild-type TNF-R1 is sufficient, like Alix overexpression, to induce massive apoptosis throughout the neural tube (data not shown). On the contrary, expression of TNF-R1ΔDD halved the number of TUNEL positive nuclei in the ventral part of the tube (Figure 9Ae,f and 9B). This, together with our demonstration that the endogenous receptor is expressed at the time of programmed cell death, indicates that activation of TNF-R1 regulates the death of cervical motoneurons. Taken together, these *in vivo* data strongly suggest that AlixΔALG-2 blocks programmed cell death by interfering with TNF-R1 death signalling.

DISCUSSION

We previously showed that overexpressed Alix is sufficient to activate caspases and apoptosis and that this activity requires binding to ALG-2. On the contrary, expression of the C-terminal half of Alix blocked apoptosis depending on its capacity to bind ALG-2, suggesting that it acts by titrating out ALG-2 (17,18). Interestingly, this truncated form of Alix accumulates in cytoplasmic inclusions which also contain ALG-2 and activated caspases (17, Chatellard-Causse *et al*., unpublished observations). Rao *et al*. have shown that ALG-2 is necessary for caspase activation following an abnormal rise in cytosolic calcium (24). Their observations suggested that ALG-2 belongs to a complex allowing caspase-9 activation following cytosolic calcium elevation due to a stress to the reticulum. Our present results demonstrate that ALG-2 can also form a complex with pro-caspase-8, independently of Alix, and that this requires the prodomain of the zymogen but not the catalytic activity of the protease.

Historically, caspase-8 was described as an initiator caspase activated by members of the TNF-R1 family of death receptors stimulating the extrinsic pathway of apoptosis (25). These latter recruit, through an 80 amino-acid long Death Domain (DD), other DD containing cytoplasmic proteins which participate in the formation of the Death Inducing Signalling Complex (DISC) recruiting and activating pro-caspase-8 or 10. We observed that the DD of TNF-R1 is mandatory for the interaction with Alix and therefore with the Alix/ALG-2 complex. The TNFα ligand is known to induce, via the intracellular domain of the receptor, the rapid formation of complex I made of the adaptor TRADD, the protein kinase RIP1 and the signal transducer TRAF2. This complex signals cell survival through JNK and IkB kinase, the latter activating transcription factor NFkB whose targets can mediate cell survival. Complex I can dissociate from the receptor and, together with the adaptor protein FADD, recruit and activate pro-caspase-8 (26). Schütze and colleagues introduced a twist to this model when they published convincing data showing that aggregation of TRADD, FADD and caspase-8 can occur on TNF-R1, but that this is critically dependent on receptor endocytosis (3). In line with this, we observed that blocking clathrin dependent endocytosis significantly inhibited apoptosis induced by TNF-R1. In their model, Schneider-Brachert *et al.* claim that TNF-R1 containing endosomes would establish the platform on which the DISC may form (3). Since Alix can bind TNF-R1, on one side, and ALG-2 which can interact with caspase-8 on the other, it may act as an adaptor for recruiting pro-caspase-8 on the surface of

TNF-R1 containing endosomes. In favour of this model, we found that binding of Alix to TNF-R1 is totally abolished upon deletion of its binding domains to CHMP-4B and Tsg-101 of ESCRT-III and ESCRT-I respectively, suggesting that stabilisation of Alix binding to the TNF-R1 complex occurs through interactions with these endosomal proteins. Furthermore we could identify TNF-R1, Alix, ALG-2, caspase-8, and FADD within a common, Triton-X100 resistant, complex in endosomal fractions containing TNFα bound to its endocytosed receptor. Thus AlixΔALG-2 may block death induced by TNF-R1 by impairing the recruitment of pro-caspase-8 onto surface of TNF-R1 containing endosomes. The protecting effect of AlixΔALG-2 is not simply due to blocking of endocytosis of the activated receptor, as this is not influenced by the mutant. Nor is it due to an impairment of the degradation of the receptor inside lysosomes since the dead version of the ATPase SKD-1, which leads to gross abnormalities in multivesicular endosomes (27), had no protecting activity against TNF-R1.

In order to verify that Alix/ALG-2 may regulate TNF-R1 induced cell death in a physiological setting, we extended our previous studies showing that AlixΔALG-2 can block the programmed cell death (PCD) of chick cervical MTN (18) by demonstrating that this phenomenon is driven by TNF-R1. Among death receptors of the TNF-R family, $P75^{NGFR}$, Fas, and TNF-R1 (28) have been postulated to play an active role during MTN developmental death. Sedel *et al*. have shown that death of E12-13 rat MTN is regulated by TNFα and that death of mouse MTN is significantly reduced in double KO for TNFα and TNF-R1(29). In the chick embryo, TNFα was detected by imunohistochemistry from HH stage 18 (E3) with a peak at HH stage 24 to 25 (E4.5 to E5) (30) and we found that TNF-R1 is transiently expressed during PCD of cervical MTN with a pattern reminiscent of that of Alix. Our demonstration that TNF-R1ΔDD impaired death of cervical MTN, in a way similar to the pan caspase inhibitor p35, DN-pro-caspase-8 or AlixΔALG-2 (18), demonstrates that TNF-R1 drives MTN PCD which is regulated by Alix/ALG-2. It is here noteworthy that CIN85, another interactor of Alix, has been reported to be involved in TNF-R1 signalling (31) and we have observed that deletion of the CIN85 binding site impairs the death blocking activity of the C-terminal half of Alix in chick MTN (Mahul-Mellier, unpublished observation).

de Gassart *et al.* have reported caspase activity in exosomes, which correspond to intralumenal vesicles of MVBs and are enriched in Alix (32). Exosomes also bear TNF-R1 indicating that the receptor is a cargo of the intralumenal vesicles, but without its interactors TRADD, RIP and TRAF2 (33). It may therefore be speculated that Alix and ALG-2 which accompany and get entrapped into vesicles budding inside MVBs could pull TNF-R1 and caspase-8 inside endosomes. This would efficiently isolate the activated caspase from its cytosolic substrates and lead to its rapid degradation inside lysosomes fusing with MVBs. Thus, one reason for why activation of pro-caspase-8 in the vicinity of Alix and ALG-2 occurs on the surface of endosomes containing TNF-R1 is that it may allow a potent control, to rapidly tune down caspase-8 activity.

As ALG-2 binding to Alix is strictly calcium-dependent, our results also beg the question of the relationship between cytosolic calcium and TNF-R1. The present literature remains controversial about the role of cytosolic calcium in TNFα induced cell death. Some investigators have failed to find evidence for a TNFα induced calcium response in U937 monocytes (34) or in KYM-1 and Hela cells overexpressing the TNF receptor (35). In contrast, Bellomo *et al.* (36) and Kong *et al* (37) found an increase in intracellular calcium using BT-20 and L929 cells, respectively. More recently, Draper *et al*. (38) found a sustained rise in cytosolic calcium following CHX/ TNFα treatment of C3HA fibroblast cells. Fas, which also requires endocytosis for caspase-8 activation, has been shown to induce calcium release from internal stores. It is also noteworthy that endosomes are known to contain high concentrations of calcium and calcium leakage from endosomes regulates their maturation (39). Thus a rise in calcium in the close vicinity of endosomes might allow ALG-2 to bind to Alix and recruit caspase-8 on the surface of endosomes. This is even more relevant knowing that Fas-mediated apoptosis requires calcium release from the endoplasmic reticulum (40) and we will now test whether

Fas-mediated cell death, also involves Alix/ALG-2 during activation of caspase-8. We will also need to examine whether the interaction of ALG-2 and Alix to pro-caspase-8 and TNF-R1, respectively, is direct or through proteins of the DISC complex. Interactions within this complex are homophilic between DD or Death Effector Domains (DED). We showed that the DD of TNF-R1 and the DED containing pro-domain of pro-caspase 8 are obligatory for binding to Alix and ALG-2 respectively, and that FADD is present in the Alix/ALG-2/pro-caspase-8 complex. Since apparently, neither Alix nor ALG-2 contain death adaptor domains, we now need to characterize the new module which allows their interaction to the DISC.

REFERENCES

1. van der Goot, F. G., and Gruenberg, J. (2006) *Trends Cell Biol* **16**(10), 514-521
2. Barker, P. A., Hussain, N. K., and McPherson, P. S. (2002) *Trends Neurosci* **25**(8), 379-381
3. Schneider-Brachert, W., Tchikov, V., Neumeyer, J., Jakob, M., Winoto-Morbach, S., Held-Feindt, J., Heinrich, M., Merkel, O., Ehrenschwender, M., Adam, D., Mentlein, R., Kabelitz, D., and Schutze, S. (2004) *Immunity* **21**(3), 415-428.
4. Williams, R. L., and Urbe, S. (2007) *Nat Rev Mol Cell Biol* **8**(5), 355-368
5. Missotten, M., Nichols, A., Rieger, K., and Sadoul, R. (1999) *Cell Death Differ* **6**(2), 124-129
6. Vito, P., Lacana, E., and D'Adamio, L. (1996) *Science* **271**, 521-525
7. Vito, P., Pellegrini, L., Guiet, C., and D'Adamio, L. (1999) *J Biol Chem* **274**(3), 1533-1540
8. Strack, B., Calistri, A., Craig, S., Popova, E., and Gottlinger, H. G. (2003) *Cell* **114**(6), 689-699.
9. von Schwedler, U. K., Stuchell, M., Muller, B., Ward, D. M., Chung, H. Y., Morita, E., Wang, H. E., Davis, T., He, G. P., Cimbora, D. M., Scott, A., Krausslich, H. G., Kaplan, J., Morham, S. G., and Sundquist, W. I. (2003) *Cell* **114**(6), 701-713.
10. Carlton, J. G., and Martin-Serrano, J. (2007) *Science* **316**(5833), 1908-1912
11. Morita, E., Sandrin, V., Chung, H. Y., Morham, S. G., Gygi, S. P., Rodesch, C. K., and Sundquist, W. I. (2007) *Embo J* **13**, 13
12. Matsuo, H., Chevallier, J., Mayran, N., Le Blanc, I., Ferguson, C., Faure, J., Blanc, N. S., Matile, S., Dubochet, J., Sadoul, R., Parton, R. G., Vilbois, F., and Gruenberg, J. (2004) *Science* **303**(5657), 531-534.
13. Chatellard-Causse, C., Blot, B., Cristina, N., Torch, S., Missotten, M., and Sadoul, R. (2002) *J Biol Chem* **277**(32), 29108-29115.
14. Chen, B., Borinstein, S. C., Gillis, J., Sykes, V. W., and Bogler, O. (2000) *J Biol Chem* **275**(25), 19275-19281.
15. Cabezas, A., Bache, K. G., Brech, A., and Stenmark, H. (2005) *J Cell Sci* **118**(Pt 12), 2625-2635
16. Schmidt, M. H., Hoeller, D., Yu, J., Furnari, F. B., Cavenee, W. K., Dikic, I., and Bogler, O. (2004) *Mol Cell Biol* **24**(20), 8981-8993. "CA-P8901-95616/CA/NCI", "CA-R95601-84109/CA/NCI" "Journal Article"
17. Trioulier, Y., Torch, S., Blot, B., Cristina, N., Chatellard-Causse, C., Verna, J. M., and Sadoul, R. (2004) *J Biol Chem* **279**(3), 2046-2052
18. Mahul-Mellier, A.-L., Hemming, F. J., Blot, B., Fraboulet, S., and Sadoul, R. (2006) *Journal of Neuroscience* **26**(2), 542-549
19. Sadoul, R. (2006) *Bio. Cell* **98**, 69-77
20. Todd, I., Radford, P. M., Draper-Morgan, K. A., McIntosh, R., Bainbridge, S., Dickinson, P., Jamhawi, L., Sansaridis, M., Huggins, M. L., Tighe, P. J., and Powell, R. J. (2004) *Immunology* **113**(1), 65-79
21. Shibata, H., Yamada, K., Mizuno, T., Yorikawa, C., Takahashi, H., Satoh, H., Kitaura, Y., and Maki, M. (2004) *J Biochem (Tokyo)* **135**(1), 117-128
22. Fraboulet, S., Hemming, F. J., Mahul, A. L., Cristina, N., and Sadoul, R. (2003) *Gene Expr Patterns* **3**(2), 139-142.

23. Bump, N. J., Hackett, M., Hugunin, M., Seshagiri, S., Brady, K., Chen, P., Ferenz, C., Franklin, S., Ghayur, T., Li, P., and et al. (1995) *Science* **269**(5232), 1885-1888
24. Rao, R. V., Poksay, K. S., Castro-Obregon, S., Schilling, B., Row, R. H., del Rio, G., Gibson, B. W., Ellerby, H. M., and Bredesen, D. E. (2004) *J Biol Chem* **279**(1), 177-187
25. Muzio, M., Chinnaiyan, A. M., Kischkel, F. C., O'Rourke, K., Shevchenko, A., Ni, J., Scaffidi, C., Bretz, J. D., Zhang, M., Gentz, R., Mann, M., Krammer, P. H., Peter, M. E., and Dixit, V. M. (1996) *Cell* **85**(6), 817-827
26. Micheau, O., and Tschopp, J. (2003) *Cell* **114**(2), 181-190
27. Fujita, H., Yamanaka, M., Imamura, K., Tanaka, Y., Nara, A., Yoshimori, T., Yokota, S., and Himeno, M. (2003) *J Cell Sci* **116**(Pt 2), 401-414
28. Raoul, C., Pettmann, B., and Henderson, C. E. (2000) *Curr Opin Neurobiol* **10**(1), 111-117
29. Sedel, F., Bechade, C., Vyas, S., and Triller, A. (2004) *J Neurosci* **24**(9), 2236-2246.
30. Wride, M. A., and Sanders, E. J. (1995) *Anat Embryol (Berl)* **191**(1), 1-10
31. Narita, T., Nishimura, T., Yoshizaki, K., and Taniyama, T. (2005) *Exp Cell Res* **304**(1), 256-264
32. de Gassart, A., Geminard, C., Fevrier, B., Raposo, G., and Vidal, M. (2003) *Blood* **102**(13), 4336-4344
33. Hawari, F. I., Rouhani, F. N., Cui, X., Yu, Z. X., Buckley, C., Kaler, M., and Levine, S. J. (2004) *Proc Natl Acad Sci U S A* **101**(5), 1297-1302
34. Hasegawa, Y., and Bonavida, B. (1989) *J Immunol* **142**(8), 2670-2676
35. McFarlane, S. M., Anderson, H. M., Tucker, S. J., Jupp, O. J., and MacEwan, D. J. (2000) *Mol Cell Biochem* **211**(1-2), 19-26
36. Bellomo, G., Perotti, M., Taddei, F., Mirabelli, F., Finardi, G., Nicotera, P., and Orrenius, S. (1992) *Cancer Res* **52**(5), 1342-1346
37. Kong, S. K., Fung, K. P., Choy, Y. M., and Lee, C. Y. (1997) *Oncology* **54**(1), 55-62
38. Draper, D. W., Harris, V. G., Culver, C. A., and Laster, S. M. (2004) *J Immunol* **172**(4), 2416-2423
39. Saito, M., Hanson, P. I., and Schlesinger, P. (2007) *J Biol Chem* **282**(37), 27327-27333
40. Wozniak, A. L., Wang, X., Stieren, E. S., Scarbrough, S. G., Elferink, C. J., and Boehning, D. (2006) *J Cell Biol* **175**(5), 709-714
41. Ferro, M., Seigneurin-Berny, D., Rolland, N., Chapel, A., Salvi, D., Garin, J., and Joyard, J. (2000) *Electrophoresis* **21**(16), 3517-3526

FOOTNOTES

The authors would like to thank Patrick Mehlen, Wulf Schneider-Brachert and Masatoshi Maki for reagents, Yves Goldberg, Karin Sadoul and Fiona Hemming for critical reading of the manuscript and numerous suggestions throughout this work, Gilles Bodon for help with the receptosome experiment and Thomas Mellier for his patience.

This work was supported in part by Inserm, the University Joseph Fourier, grants from the "Association Française contre les Myopathies" and from the "Association pour la recherche sur la sclérose latérale amyotrophique". ALM was supported by a fellowship from AFM.

The abbreviations used are: ALG-2, Apoptosis Linked gene-2; Alix, ALG-2 interacting protein X; CHMP-4B, CHarged Multivesicular body Proteins-4B; CIN85, Cbl-interacting 85-kDa protein; DD, Death Domain; DED, Death Effector Domain; ESCRT, Endosomal Sorting Complex Required for Transport; HH, Hamburger-Hamilton stage; MVB, MultiVesicular Body; Tsg101, Tumor Susceptibility Gene 101; TNF, Tumor Necrosis Factor; TNF-R1, Tumor Necrosis Factor-Receptor 1; TUNEL, Terminal Transferase dUTP Nick End-Labelling

FIGURE LEGENDS

Fig. 1: Schematic representation of Alix pro-caspase-8 and TNF-R1 and their mutants used throughout this study

Fig. 2: Alix co-immunoprecipitates with DN-pro-caspase-8.
A. Alix/pro-caspase-8 co-immunoprecipitation (IP) requires calcium.
BHK cells co-expressing Flag-Alix and HA-DN-pro-caspase-8 were lysed and immunoprecipitated with anti-HA antibody in RIPA buffer supplemented or not with 1 mM $CaCl_2$. Immunoprecipitates were blotted and analysed with polyclonal antibodies agains Alix (lower) and against HA (upper panel).
B. Co-IP of Alix with DN-pro-caspase-8 requires the pro-domain of the zymogen.
BHK cells co-expressing Flag-Alix together with HA-DN-pro-caspase-8 or HA-DN-caspase-8-ΔDED were lysed and immunoprecipitated with anti-HA in RIPA containing 1 mM $CaCl_2$ (CaRIPA) and analysed as in A.
C. Endogenous ALG-2 is detected in pro-caspase-8/ Alix co-immunoprecipitates.
BHK cells co-expressing Flag-Alix together with HA-DN-pro-caspase-8 were lysed and immunoprecipitated as in B; immunoprecipitates were analysed by Western Blot (WB) with polyclonal anti HA , anti-ALG-2 and anti-Flag antibodies (from top to bottom).

Fig. 3: ALG-2 co-immunoprecipitates with DN-pro-caspase-8.
A. ALG-2/pro-caspase-8 co-IP requires calcium.
BHK cells co-expressing Flag-ALG-2 and HA-DN-pro-caspase-8 were lysed and immunoprecipitated with anti HA in RIPA (ϕ), or RIPA containing either 3 mM EGTA or 1 mM $CaCl_2$. Immunoprecipitates were analysed using polyclonal antibodies against HA (upper) and Flag (lower panel).
B. Co-IP of ALG-2 with DN-pro-caspase-8 requires the pro-domain of the zymogen.
BHK cells co-expressing Flag-ALG-2 together with HA-DN-pro-caspase-8 or HA-DN-caspase-8-ΔDED were lysed and immunoprecipitated with anti HA in CaRIPA and analysed as in A.
C. Co-IP of Alix with DN-pro-caspase-8 requires its ALG-2 binding domain.
BHK cells were co-transfected with either Flag-Alix WT or Flag-AlixΔALG-2 and HA-DN-pro-caspase-8. IP with anti-HA antibody were performed in CaRIPA. Immunoprecipitates were analysed by WB using polyclonal antibodies against HA (upper) and Alix (lower panel).
D. ALG-2 co-immunoprecipitates with DN-pro-caspase-8 in cells depleted of Alix.
BHK cells expressing shAlix to down-regulate expression of the protein were transfected with Flag-ALG-2 and HA-DN-pro-caspase-8 lysed in CaRIPA and immunoprecipitated with an anti-HA antibody. Immunoprecipitates were analysed by WB using anti-Flag (lower) and HA polyclonal antibodies (upper panel). Right insert: Western blot analysis of lysates using a polyclonal antibody anti-Alix and a monoclonal anti-actin shows the decrease of endogenous Alix expression in BHK shAlix cells.

Fig. 4: Alix co-immunoprecipitates with TNF-R1.
A. Co-IP of overexpressed Alix and TNF-R1. RIPA lysates of HEK 293 cells co-expressing Flag-Alix and TNF-R1 were immunoprecipitated with anti-Flag antibodies and blots probed with anti-Alix (upper) and anti-TNF-R1 (lower panel).
B. Co-IP of endogenous Alix and TNF-R1.
RIPA lysates of Hela cells were immunoprecipitated using a polyclonal anti-TNF-R1. The IP was analysed by WB using a monoclonal antibody against human Alix.
C. Co-IP of Alix with TNF-R1 requires the death domain of the receptor.
RIPA lysates of HEK 293 cells co-expressing Flag-Alix and TNF-R1 deleted from its death domain (TNF-R1ΔDD) were immunoprecipitated with anti-Flag or with anti-TNF-R1 and blots probed with the appropriate polyclonal antibodies as in A
D. Co-immunoprecipitation of Alix with TNF-R1 requires its binding site to Tsg101 and Bro1 but not to ALG-2.
Cells co-expressing TNF-R1 and either Flag-AlixΔTsg101, Flag-AlixΔBro1 or Flag-AlixΔALG-2 were solubilised in RIPA and total lysates immunoprecipitated with anti-Flag; Western blots were probed with the appropriate polyclonal antibodies as in A and C.

Fig. 5: ALG-2 co-IP with TNF-R1 requires its capacity to bind calcium.
A. ALG-2 co-IP with TNF-R1 and Alix. HEK293 cells were co-transfected with Flag-ALG-2 and TNF-R1. RIPA cell lysates were immunoprecipitated with anti-Flag or with anti-TNF-R1 and blots probed with the appropriate antibodies. Lower panel shows the presence of endogenous Alix within the immunoprecipitates as revealed with an anti-Alix antibody.
B. Calcium binding-deficient ALG-2 mutant does not co-IP with Alix (a) or with TNF-R1 (b). HEK293 co-expressing Flag-Alix a) or TNF-R1 b) together with Flag-ALG-2ΔEF^{1,3} , a point mutant unable to bind Ca^{2+}, were solubilised and immunoprecipitated in CaRIPA; Western blots were probed with the appropriate polyclonal antibodies.

Fig. 6: Alix and ALG-2 are present with pro-caspase-8 and FADD on TNF receptosomes.
A. Western blot analysis of Flag-TNFα containing endosomes prepared from HEK 293, over-expressing TNF-R1 and Myc-Alix.
0: Cells maintained at 4°C were washed with EDTA prior to endosome preparation. 30: cells incubated for 30 minutes at 37°C to induce endocytosis of TNFα bound to TNF-R1 before lysis. Magnet-isolated endosomes were run on SDS PAGE and immuno-blotted to reveal the presence of EEA1 (early endosomes), LAMP1 (late endosomes and lysosomes), GM130 (cis-Golgi) or HSP70 (mitochondria).
B. Solubilisation of TNF-R1 receptosomes leaves intact a complex containing Alix, ALG-2, FADD and pro-caspase-8.
TNF-R1 receptosomes prepared as in A were solubilised on the affinity column using 0.5 % Triton-X100 and analysed by Western blotting using the appropriate antibodies. The lack of EEA1 and LAMP1 confirms membrane solubilisation of TNF receptosomes.

Fig. 7: AlixΔALG-2 protects HEK293 from TNF-R1-induced cell death without impairing internalisation of the receptor.
A. TNF-R1 overexpression triggers apoptosis which is inhibited by AlixΔALG-2 but not by AlixΔTsg101 or SKD1 DN.
a-b: HEK 293 cells transfected with expression vectors coding for RFP or TNF-R1 and the indicated proteins. Viability was scored on the basis of nuclear morphology; cells with condensed or fragmented nuclei were counted as dead. Values are the means +/- SD of dying cells from three independent experiments. **t test, $p<0.001$.
B. MTT metabolic colorimetric test confirms the protective effect of AlixΔALG-2. Each value represents the mean +/- SD of triplicate wells from three independent experiments. **t test, $p<0.001$.
C. TNF-R1/TNFα internalisation is impaired by a dominant negative form of dynamin but not by Alix or AlixΔALG-2.
TNF-R1 internalisation was analysed using [^{125}I]-TNFα in TNF-R1 expressing cells. Each point represents the mean +/- SD of triplicate wells from three independent experiments. **t test, $p<0.001$.

Fig. 8: TNF-R1 is expressed during chick neural tube development.
A. RT-PCR analysis shows gene expression in whole extracts from chick embryos from HH stage 16 to HH stage 27.
B. Polyclonal anti-TNF-R1 recognises a main band at 55 kDa in HEK cells and a doublet with the lower band corresponding to 55 kDa in DF1 chick fibroblasts. A similar pattern is observed in chick embryo extracts (21HH, 24HH).
C-D. Cross sections of HH stage 21 (C) or 24 (D) chick embryo neural tubes immunostained with polyclonal anti-TNF-R1. Scale bar = 50 μm.

Fig. 9: TNF-R1 is involved in early cell death of cervical motoneurons.
A: Cross sections of HH stage 24 chick embryo neural tubes electroporated with pCAGGS expression vectors coding for: (a, b) GFP-p35; (c, d) DN-pro-caspase-8; (e, f) TNFR1ΔDD-

YFP; a, c, e: GFP expression 48 h after electroporation. b, d, f: TUNEL labelling of adjacent sections. Scale bar = 50 μm.
B: Ratio of TUNEL-positive cells in the electroporated versus non-electroporated side of the neural tube. Mean numbers +/- SD of TUNEL-positive cells in the neural tube of electroporated embryos, n= number of sections analysed; twelve sections per embryo were counted. **t test, $p<0.001$.

Figure 1

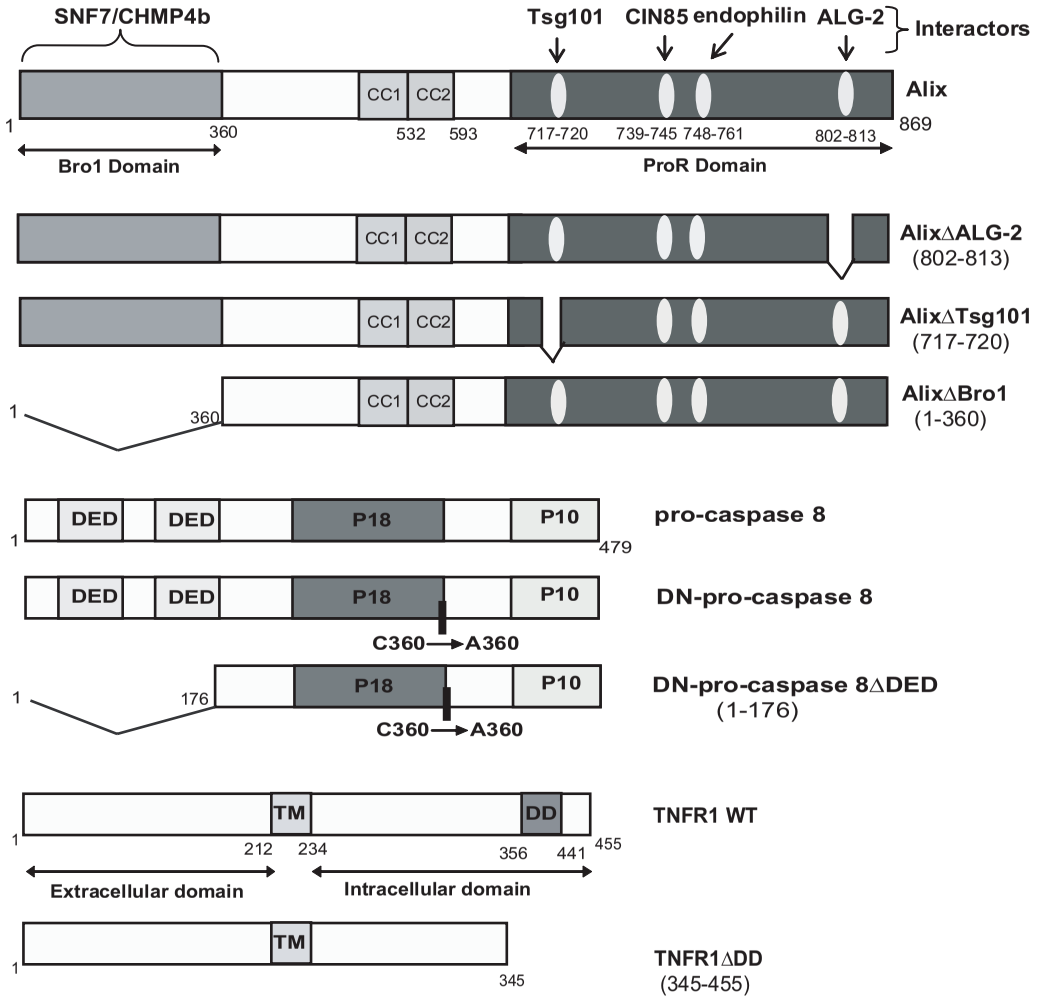
SNF7/CHMP4b
Tsg101
CIN85
endophilin
ALG-2
Interactors
Alix
CC1
CC2
1
360
532
593
717-720
739-745
748-761
802-813
869
Bro1 Domain
ProR Domain
AlixΔALG-2
(802-813)
AlixΔTsg101
(717-720)
AlixΔBro1
(1-360)
DED
DED
P18
P10
pro-caspase 8
479
DN-pro-caspase 8
C360→A360
DN-pro-caspase 8ΔDED
(1-176)
176
TM
DD
TNFR1 WT
212
234
356
441
455
Extracellular domain
Intracellular domain
TNFR1ΔDD
(345-455)
345

Figure 2

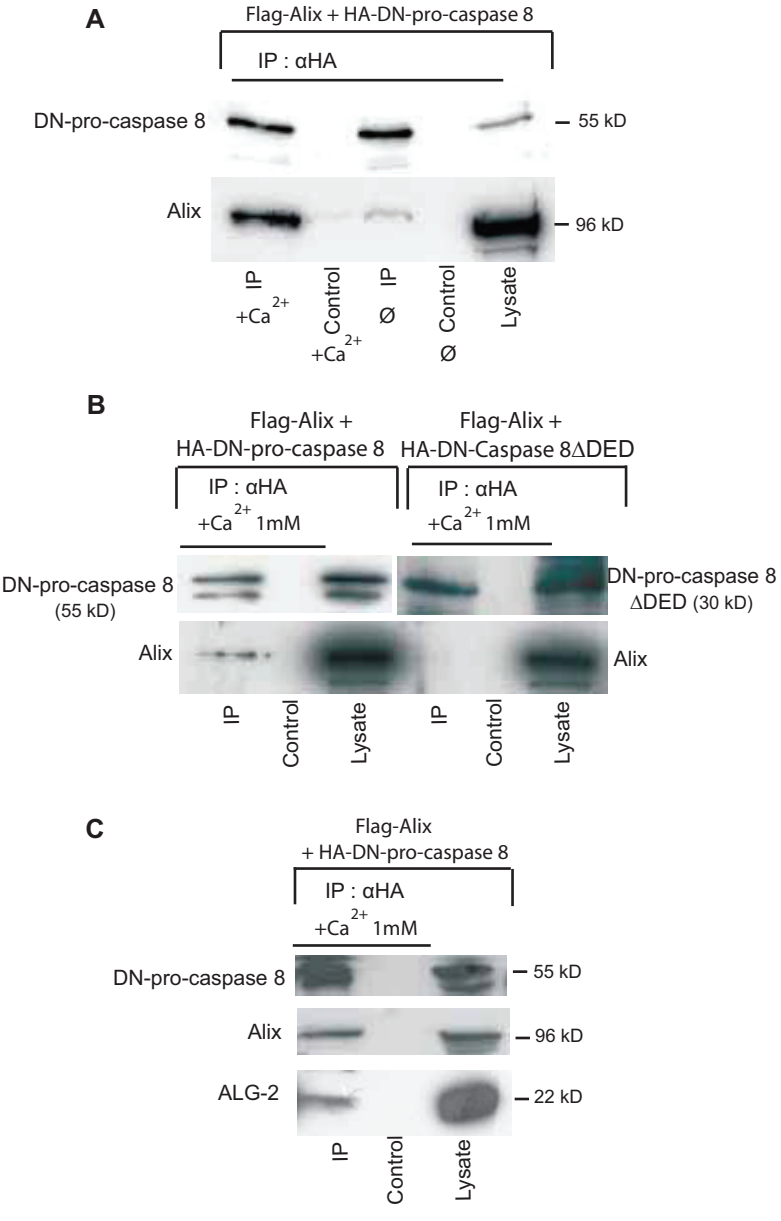
A
Flag-Alix + HA-DN-pro-caspase 8
IP : αHA
DN-pro-caspase 8
55 kD
Alix
96 kD
IP +Ca2+
Control +Ca2+
IP Ø
Control Ø
Lysate
B
Flag-Alix + HA-DN-pro-caspase 8
Flag-Alix + HA-DN-Caspase 8ΔDED
IP : αHA +Ca2+ 1mM
IP : αHA +Ca2+ 1mM
DN-pro-caspase 8 (55 kD)
DN-pro-caspase 8 ΔDED (30 kD)
Alix
Alix
IP
Control
Lysate
IP
Control
Lysate
C
Flag-Alix + HA-DN-pro-caspase 8
IP : αHA +Ca2+ 1mM
DN-pro-caspase 8
55 kD
Alix
96 kD
ALG-2
22 kD
IP
Control
Lysate

Figure 3

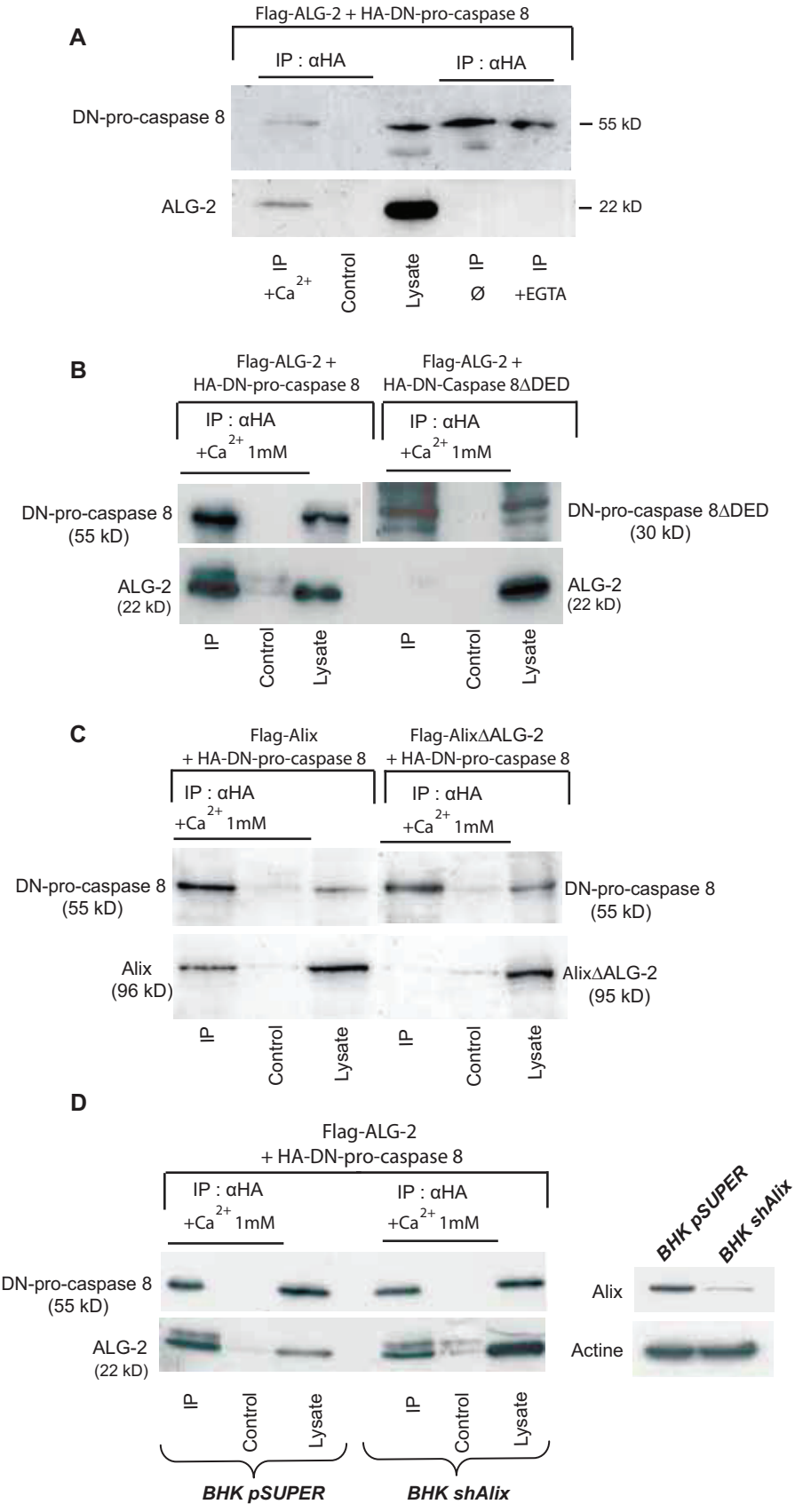
A
Flag-ALG-2 + HA-DN-pro-caspase 8
IP : αHA
IP : αHA
DN-pro-caspase 8
55 kD
ALG-2
22 kD
IP +Ca2+
Control
Lysate
IP Ø
IP +EGTA
B
Flag-ALG-2 + HA-DN-pro-caspase 8
Flag-ALG-2 + HA-DN-Caspase 8ΔDED
IP : αHA +Ca2+ 1mM
IP : αHA +Ca2+ 1mM
DN-pro-caspase 8 (55 kD)
DN-pro-caspase 8ΔDED (30 kD)
ALG-2 (22 kD)
ALG-2 (22 kD)
IP
Control
Lysate
IP
Control
Lysate
C
Flag-Alix + HA-DN-pro-caspase 8
Flag-AlixΔALG-2 + HA-DN-pro-caspase 8
IP : αHA +Ca2+ 1mM
IP : αHA +Ca2+ 1mM
DN-pro-caspase 8 (55 kD)
DN-pro-caspase 8 (55 kD)
Alix (96 kD)
AlixΔALG-2 (95 kD)
IP
Control
Lysate
IP
Control
Lysate
D
Flag-ALG-2 + HA-DN-pro-caspase 8
IP : αHA +Ca2+ 1mM
IP : αHA +Ca2+ 1mM
BHK pSUPER
BHK shAlix
DN-pro-caspase 8 (55 kD)
ALG-2 (22 kD)
Alix
Actine
IP
Control
Lysate
IP
Control
Lysate
BHK pSUPER
BHK shAlix

Figure 4

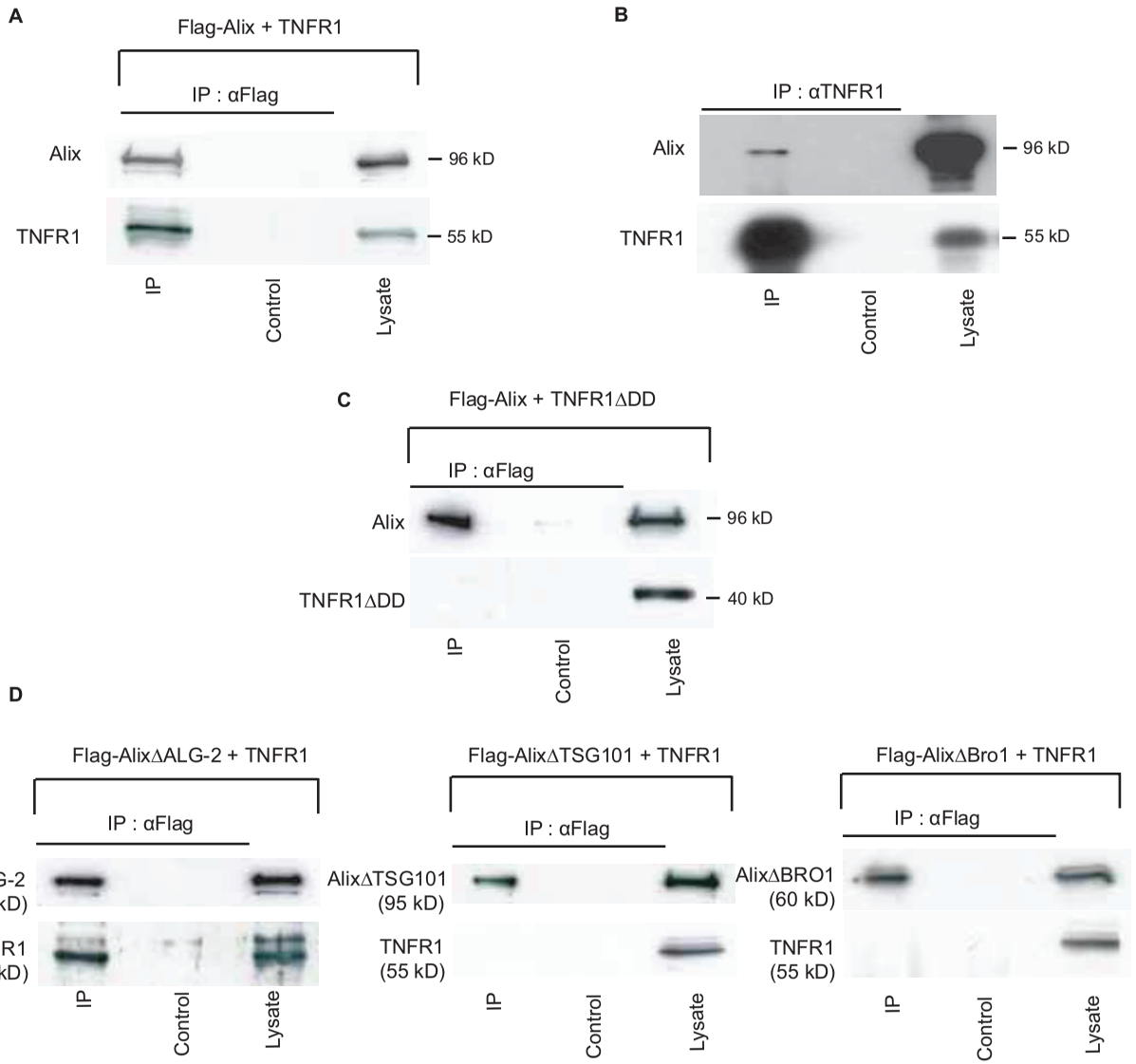
A
Flag-Alix + TNFR1
IP : αFlag
Alix
TNFR1
96 kD
55 kD
IP
Control
Lysate
B
IP : αTNFR1
Alix
TNFR1
96 kD
55 kD
IP
Control
Lysate
C
Flag-Alix + TNFR1ΔDD
IP : αFlag
Alix
TNFR1ΔDD
96 kD
40 kD
IP
Control
Lysate
D
Flag-AlixΔALG-2 + TNFR1
IP : αFlag
AlixΔALG-2
(95 kD)
TNFR1
(55 kD)
IP
Control
Lysate
Flag-AlixΔTSG101 + TNFR1
IP : αFlag
AlixΔTSG101
(95 kD)
TNFR1
(55 kD)
IP
Control
Lysate
Flag-AlixΔBro1 + TNFR1
IP : αFlag
AlixΔBRO1
(60 kD)
TNFR1
(55 kD)
IP
Control
Lysate

Figure 5

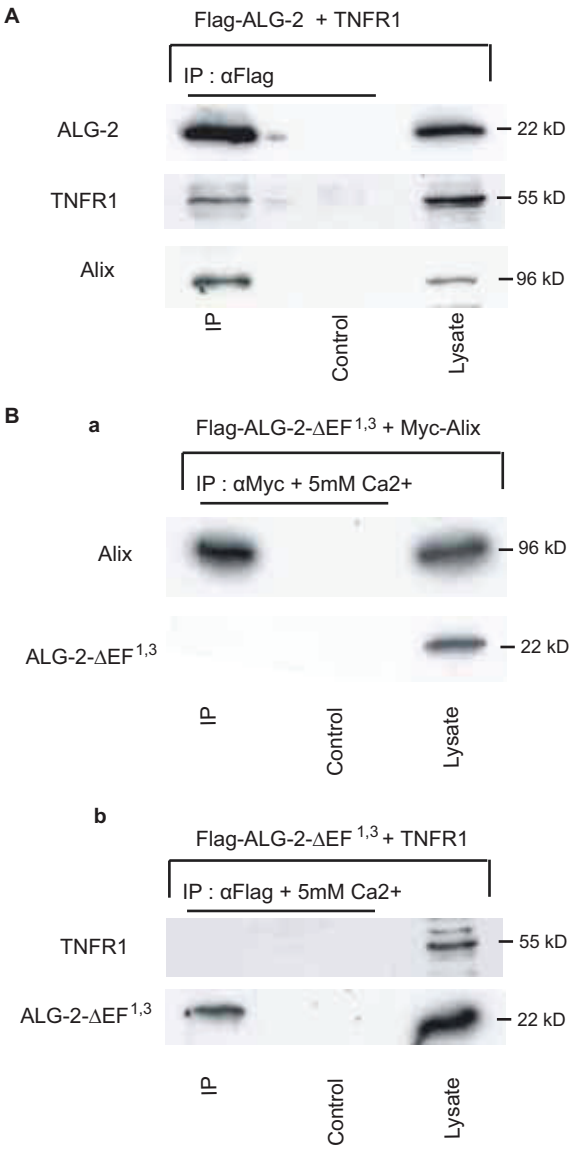
A
Flag-ALG-2 + TNFR1
IP : αFlag
ALG-2
TNFR1
Alix
22 kD
55 kD
96 kD
IP
Control
Lysate
B
a
Flag-ALG-2-ΔEF 1,3 + Myc-Alix
IP : αMyc + 5mM Ca2+
Alix
ALG-2-ΔEF 1,3
96 kD
22 kD
IP
Control
Lysate
b
Flag-ALG-2-ΔEF 1,3 + TNFR1
IP : αFlag + 5mM Ca2+
TNFR1
ALG-2-ΔEF 1,3
55 kD
22 kD
IP
Control
Lysate

Figure 6

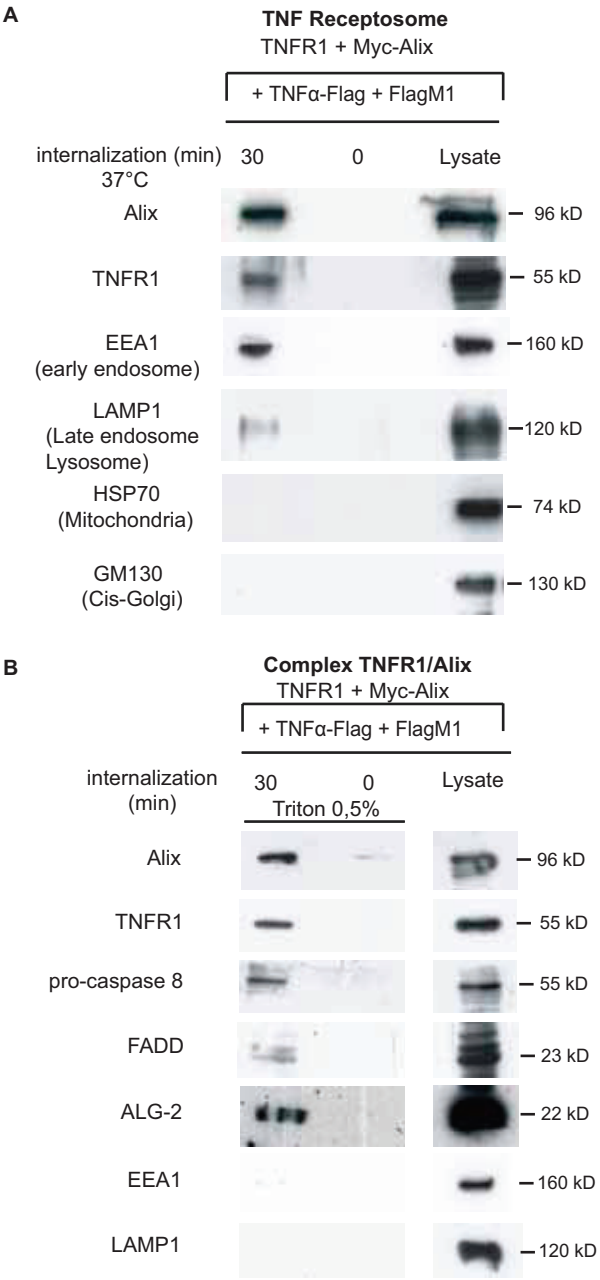
A
TNF Receptosome
TNFR1 + Myc-Alix
+ TNFα-Flag + FlagM1
internalization (min)
37°C
30
0
Lysate
Alix
96 kD
TNFR1
55 kD
EEA1
(early endosome)
160 kD
LAMP1
(Late endosome
Lysosome)
120 kD
HSP70
(Mitochondria)
74 kD
GM130
(Cis-Golgi)
130 kD
B
Complex TNFR1/Alix
TNFR1 + Myc-Alix
+ TNFα-Flag + FlagM1
internalization
(min)
30
0
Triton 0,5%
Lysate
Alix
96 kD
TNFR1
55 kD
pro-caspase 8
55 kD
FADD
23 kD
ALG-2
22 kD
EEA1
160 kD
LAMP1
120 kD

Figure 7

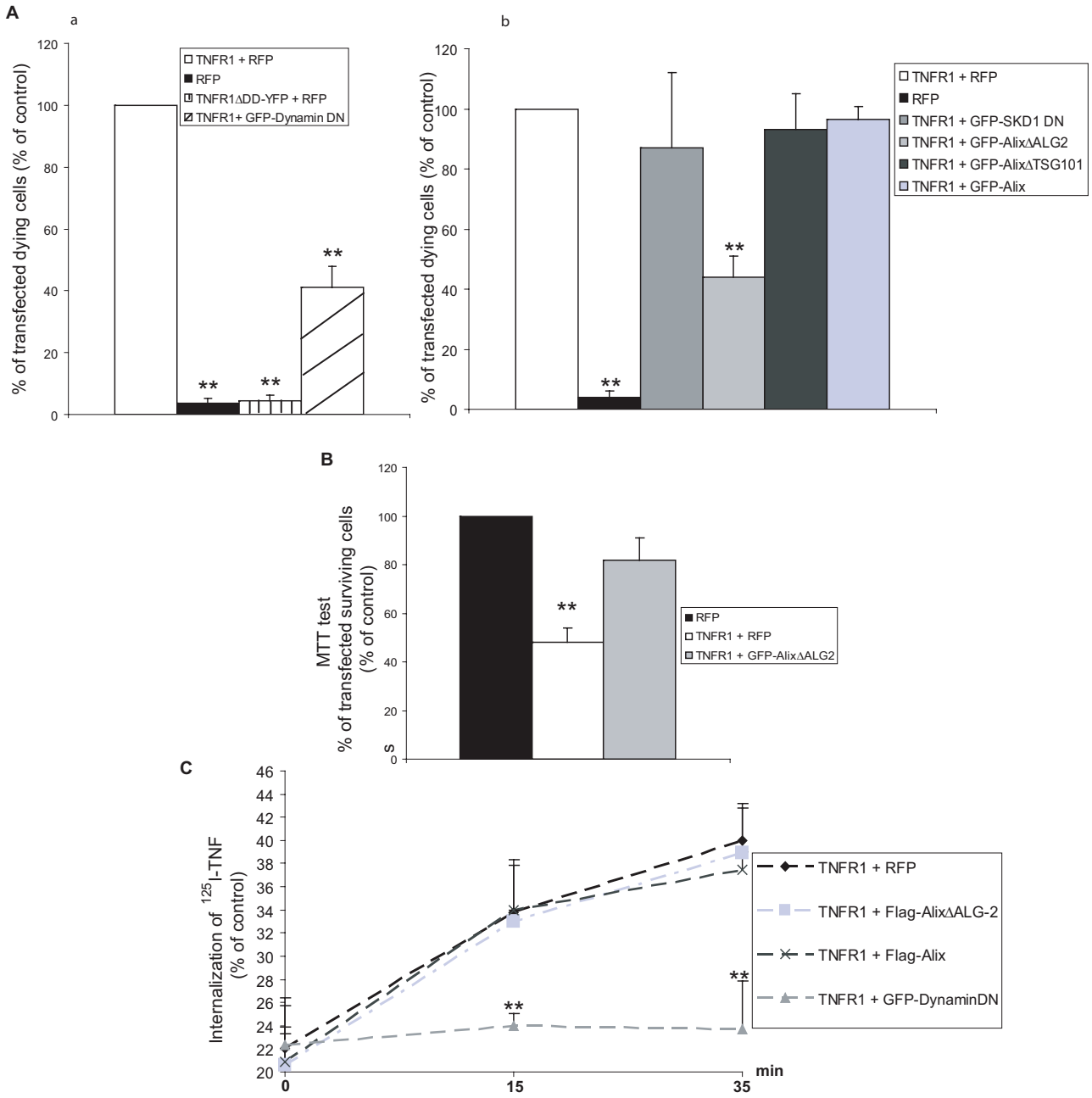
A
a
% of transfected dying cells (% of control)
TNFR1 + RFP
RFP
TNFR1ΔDD-YFP + RFP
TNFR1+ GFP-Dynamin DN
b
% of transfected dying cells (% of control)
TNFR1 + RFP
RFP
TNFR1 + GFP-SKD1 DN
TNFR1 + GFP-AlixΔALG2
TNFR1 + GFP-AlixΔTSG101
TNFR1 + GFP-Alix
B
MTT test
% of transfected surviving cells
(% of control)
RFP
TNFR1 + RFP
TNFR1 + GFP-AlixΔALG2
C
Internalization of 125I-TNF
(% of control)
TNFR1 + RFP
TNFR1 + Flag-AlixΔALG-2
TNFR1 + Flag-Alix
TNFR1 + GFP-DynaminDN
min

Figure 8

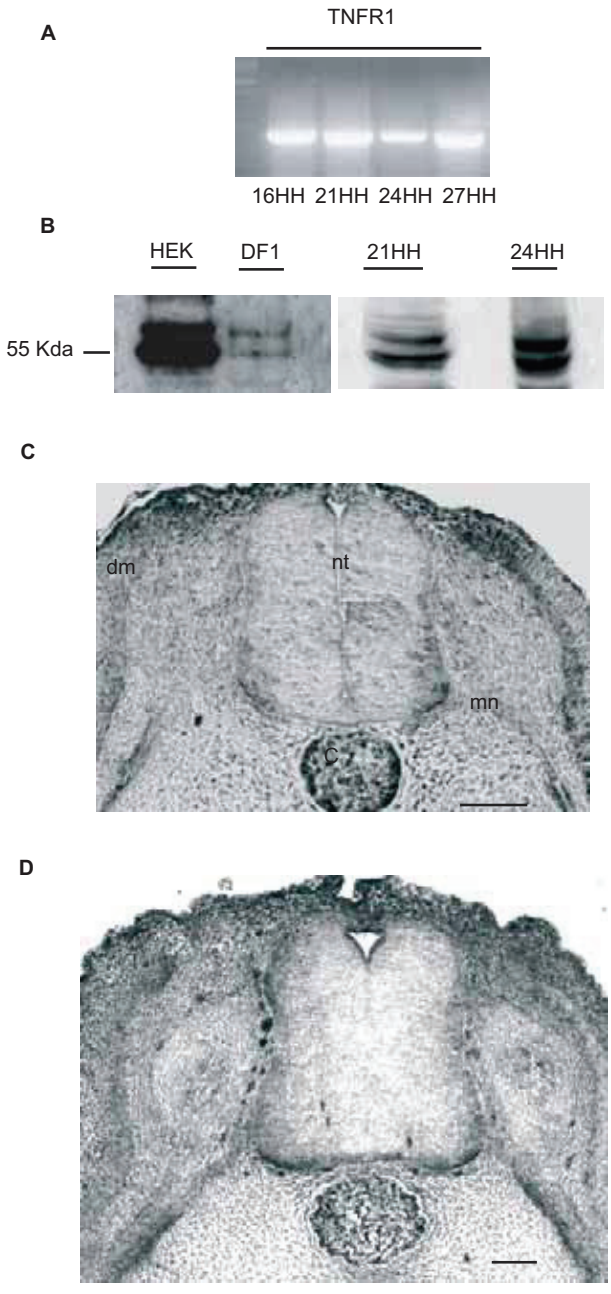
A
TNFR1
16HH 21HH 24HH 27HH
B
HEK
DF1
21HH
24HH
55 Kda
C
dm
nt
mn
C
D

Figure 9

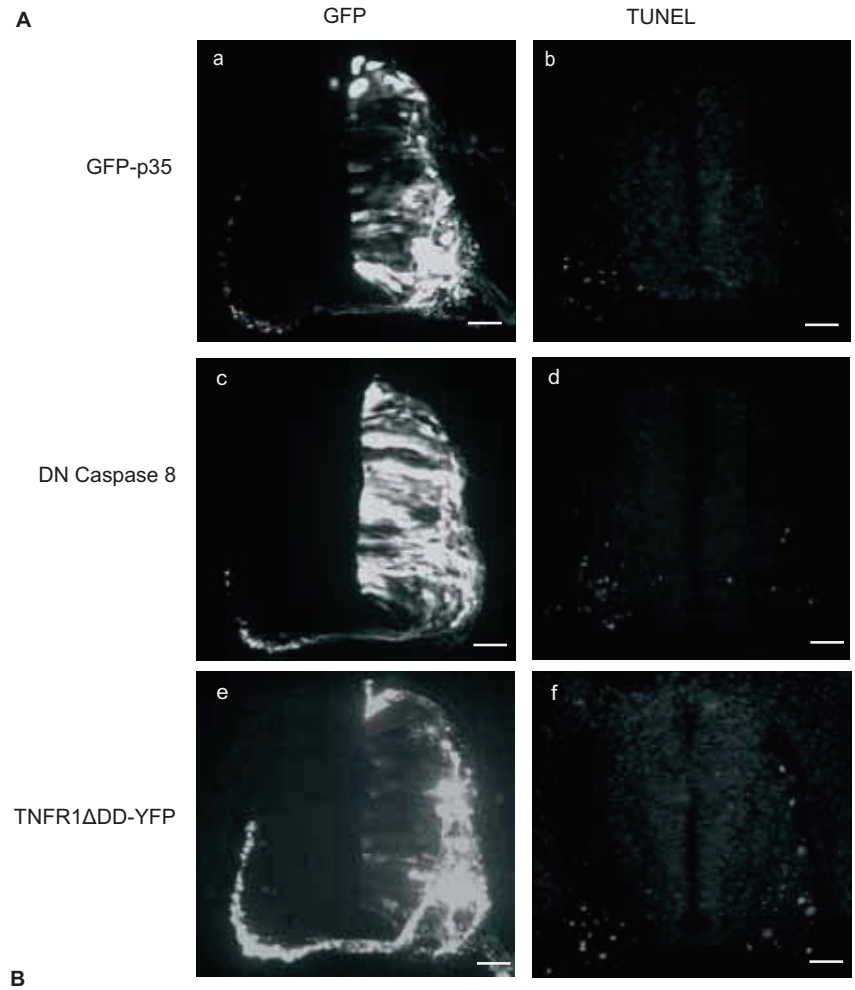
A
GFP
TUNEL
a
b
GFP-p35
c
d
DN Caspase 8
e
f
TNFR1ΔDD-YFP
B
Numbers of TUNEl positive cells
Electroporated side/Non electroporated side
1,2
1
0,8
0,6
0,4
0,2
0
**
**
**
n=168
n=156
n=156
n=156
GFP
GFP-P35
DN Caspase 8
TNFR1ΔDD-YFP